

# FOXL1 Regulates Lung Fibroblast Function via Multiple Mechanisms

Naoya Miyashita<sup>1</sup>, Masafumi Horie<sup>2</sup>, Hiroshi I. Suzuki<sup>3,4</sup>, Minako Saito<sup>1</sup>, Yu Mikami<sup>1,5</sup>, Kenichi Okuda<sup>1,5</sup>, Richard C. Boucher<sup>5</sup>, Maho Suzukawa<sup>6</sup>, Akira Hebisawa<sup>6</sup>, Akira Saito<sup>1,7</sup>, and Takahide Nagase<sup>1</sup>

<sup>1</sup>Department of Respiratory Medicine, Graduate School of Medicine, and <sup>7</sup>Division for Health Service Promotion, The University of Tokyo, Tokyo, Japan; <sup>2</sup>Department of Cancer Genome Informatics, Graduate School of Medicine, Osaka University, Osaka, Japan; <sup>3</sup>David H. Koch Institute for Integrative Cancer Research, Massachusetts Institute of Technology, Cambridge, Massachusetts; <sup>4</sup>Division of Molecular Oncology, Center for Neurological Diseases and Cancer, Graduate School of Medicine, Nagoya University, Nagoya, Japan; <sup>5</sup>Marsico Lung Institute/Cystic Fibrosis Research Center, University of North Carolina at Chapel Hill, Chapel Hill, North Carolina; and <sup>6</sup>National Hospital Organization Tokyo National Hospital, Tokyo, Japan

ORCID ID: 0000-0002-0184-1376 (A.S.).

## Abstract

Fibroblasts provide a structural framework for multiple organs and are essential for wound repair and fibrotic processes. Here, we demonstrate functional roles of FOXL1 (forkhead box L1), a transcription factor that characterizes the pulmonary origin of lung fibroblasts. We detected high *FOXL1* transcripts associated with DNA hypomethylation and super-enhancer formation in lung fibroblasts, which is in contrast with fibroblasts derived from other organs. RNA *in situ* hybridization and immunohistochemistry in normal lung tissue indicated that FOXL1 mRNA and protein are expressed in submucosal interstitial cells together with airway epithelial cells. Transcriptome analysis revealed that FOXL1 could control a broad array of genes that potentiate fibroblast function,

including TAZ (transcriptional coactivator with PDZ-binding motif)/YAP (Yes-associated protein) signature genes and PDGFR $\alpha$  (platelet-derived growth factor receptor- $\alpha$ ). *FOXL1* silencing in lung fibroblasts attenuated cell growth and collagen gel contraction capacity, underscoring the functional importance of FOXL1 in fibroproliferative reactions. Of clinical importance, increased *FOXL1* mRNA expression was found in fibroblasts of idiopathic pulmonary fibrosis lung tissue. Our observations suggest that FOXL1 regulates multiple functional aspects of lung fibroblasts as a key transcription factor and is involved in idiopathic pulmonary fibrosis pathogenesis.

**Keywords:** fibroblast; FOXL1; cap analysis of gene expression; super-enhancer; idiopathic pulmonary fibrosis

Fibroblasts are ubiquitous mesenchymal cells that regulate extracellular matrix (ECM) turnover, support the structural framework of various tissues, and modulate cell–cell or cell–ECM interactions, thereby playing a crucial role in wound healing and tissue regeneration (1). Fibroblast populations are heterogeneous (2) and display different gene expression patterns in different organs (3, 4).

We previously analyzed transcriptome data from 45 primary cultured human fibroblast lines derived from different organs and identified 14 transcription factors that showed significantly higher expression in lung-derived fibroblast lines (5). We also determined that eight of these transcription factors, including *TBX4* (T-box transcription factor 4), are associated with super-enhancers crucial for the establishment of

cell identity (6–8). Of these genes, we focused on *FOXL1* (forkhead box L1) in the present study and analyzed its functional roles in lung fibroblasts.

FOXL1 is an evolutionarily conserved transcription factor of the FOX gene family containing a winged helix DNA-binding domain (9). *FOXL1* is located in the FOX gene cluster on chromosome 16q24.1, which also contains *FOXC2* and *FOXF1*.

(Received in original form November 7, 2019; accepted in final form September 17, 2020)

Supported by JSPS (Japanese Society for the Promotion of Science) KAKENHI grants 19K23981 (N.M.), 18K08170 (A.S.), and 16H02653 (T.N.). The RNA *in situ* hybridization experiment was supported in part by the Cystic Fibrosis Foundation (grant OKUDA19I0) and a research grant from Cystic Fibrosis Research Incorporation.

Author Contributions: Conception and design: N.M., M.H., H.I.S., and A.S. Analysis and interpretation: N.M., M.H., H.I.S., M. Saito, Y.M., K.O., M. Suzukawa, and A.S. Drafting the manuscript: N.M. and A.S. Supervision: R.C.B., A.H., and T.N.

Correspondence and requests for reprints should be addressed to Akira Saito, M.D., Ph.D., Department of Respiratory Medicine, Graduate School of Medicine, The University of Tokyo, 7-3-1 Hongo, Bunkyo-ku, Tokyo 113-0033, Japan. E-mail: asaitou-tky@umin.ac.jp.

This article has a related editorial.

This article has a data supplement, which is accessible from this issue's table of contents at [www.atsjournals.org](http://www.atsjournals.org).

Am J Respir Cell Mol Biol Vol 63, Iss 6, pp 831–842, Dec 2020

Copyright © 2020 by the American Thoracic Society

Originally Published in Press as DOI: 10.1165/rcmb.2019-0396OC on September 18, 2020

Internet address: [www.atsjournals.org](http://www.atsjournals.org)

Early investigations of mouse fetal development demonstrated that *Foxl1* (the mouse homolog of *FOXL1*) is expressed in the mesenchyme surrounding the anterior gut and lung (10). Targeted disruption of *Foxl1* in mice led to aberrant cell positioning, dysregulated epithelial proliferation, and distorted tissue architecture of the stomach and small intestine, indicating its essential role in the development of the gastrointestinal tract (11). One possible mechanism for the gastrointestinal defects was the reduced expression of *Bmp2* (bone morphogenetic protein 2) and *Bmp4* observed in *Foxl1*-deficient mice (11). More recently, it was demonstrated that *Foxl1*-positive subepithelial fibroblasts constitute the intestinal stem cell niche that produces Wnt signals and maintains intestinal stem cells (12, 13).

According to gene expression profiling databases, *FOXL1* is expressed in multiple human organs at the transcript level. Although *FOXL1* is expressed in the human lung (14), its significance in lung physiology has not been explored, and it remains uncertain whether *FOXL1* is functionally relevant as a transcription factor in human lung fibroblasts.

Recent advances in lineage tracing in mice have revealed that fibroblasts regulate alveolar epithelial cell growth and differentiation (15), and PDGF-A (platelet-derived growth factor A)/PDGFR $\alpha$  (PDGF receptor- $\alpha$ ) signaling is required for alveologenesis (16). Most recently, single-cell RNA-seq (RNA-sequencing) studies identified an Axin2<sup>+</sup>Pdgfra<sup>+</sup> mesenchymal cell subpopulation that supports lung regeneration (17). In analogy with the intestinal tract, *FOXL1*-positive fibroblasts in the lungs may be involved in epithelial cell growth and differentiation (12, 13).

In addition to physiological roles in tissue homeostasis, lung fibroblasts play central roles in the pathogenesis of pulmonary diseases (18). In particular, lung fibroblasts are key effector cells of fibrotic responses in idiopathic pulmonary fibrosis (IPF) (19, 20), a chronic fibrosing interstitial pneumonia of unknown cause with a median survival of 2–4 years (21). Pathological features of IPF include alveolar epithelial regenerative failure, accumulation of

activated fibroblasts, and remodeling of the ECM (22). It is believed that clusters of fibroblasts, termed “fibroblastic foci,” are responsible for the fibrotic processes in IPF lung tissue (23).

TAZ (transcriptional coactivator with PDZ binding motif) and its homolog YAP (Yes-associated protein) are downstream effectors of the Hippo pathway. They interact with TEA domain (TEAD) family transcription factors in the nucleus to activate genes associated with cell proliferation and differentiation (24). We previously reported that TAZ is highly expressed in the fibroblastic foci of IPF lung tissue (25). We further showed that TAZ regulates a subset of profibrotic genes, including *CTGF* (connective tissue growth factor), in lung fibroblasts (25).

In the present study, we determined that *FOXL1* mRNA is highly expressed in lung fibroblasts, possibly through epigenetic mechanisms, and demonstrated that *FOXL1* controls cell growth and collagen gel contraction capacity. Transcriptome analysis revealed that *FOXL1* could regulate an array of genes important for fibroblast function, including BMP ligands, PDGFR $\alpha$ , and TAZ/YAP signature genes such as *CTGF*. Of pathological importance, we identified increased *FOXL1* expression in fibroblasts of IPF lung tissue, suggesting its involvement in IPF pathogenesis.

## Materials and Methods

### Public Data

Public datasets used in this study are summarized in Table E1 in the data supplement. Mapped sequence data were visualized using Integrative Genomics Viewer (26). DAVID 6.8 functional annotation tool was used for gene ontology analysis. Gene set enrichment analysis was performed as described previously (27). Single-cell RNA-seq data were reanalyzed using Seurat version 3 (17, 28). Identification of super-enhancers (8) and visualization of ChIP-seq (chromatin immunoprecipitation-sequencing) profiles were performed as previously described (5–7).

### Cell Cultures

The protocol of lung fibroblast isolation was approved by the University of Tokyo Ethics

Committee or by the National Hospital Organization Tokyo National Hospital Institutional Review Board (5). All patients gave written informed consent. Lung tissue was cut into 1-mm<sup>3</sup> fragments aseptically, and fibroblasts proliferating from these specimens were grown to 80% confluence and then passaged. Lung fibroblast lines derived from patients with IPF were purchased from Lonza. Details are shown in Table E2.

### Knockdown of *FOXL1*

siRNA against human *FOXL1* (Silencer Select siRNA) was purchased from Life Technologies (Table E3). Cells were transfected with 20 nM siRNA using Lipofectamine RNAiMAX (Life Technologies).

### RNA-Seq Analysis

RNA-seq reads were analyzed using CLC Genomics workbench software (Qiagen) (5). The data are deposited in the Gene Expression Omnibus database (GSE137823). Motif analysis was performed using the HOMER findMotifs.pl program (5).

### Quantitative RT-PCR

Detailed procedures were described previously (29). PCR primers are shown in Table E3.

### Immunoblot Analysis

Detailed procedures were described previously (29). Mouse monoclonal antibodies for  $\alpha$ -tubulin, CTGF, and PDGFR $\alpha$  were from Sigma-Aldrich, Santa Cruz Biotechnology, and Cell Signaling, respectively.

### Collagen Gel Contraction Assay

Three-dimensional collagen gel cultures were carried out as described previously (30).

### Migration Assay

A thin-membrane 96-well plate ChemoTx chemotaxis system (#116-8; Neuro Probe Inc.) was used. The migrated cells were treated with WST-8 solution (Nacalai Tesque).

### Human Tissue Samples and Immunohistochemistry

Formalin-fixed paraffin-embedded human lung tissue samples (Table E4) were used for immunohistochemistry. The protocol was

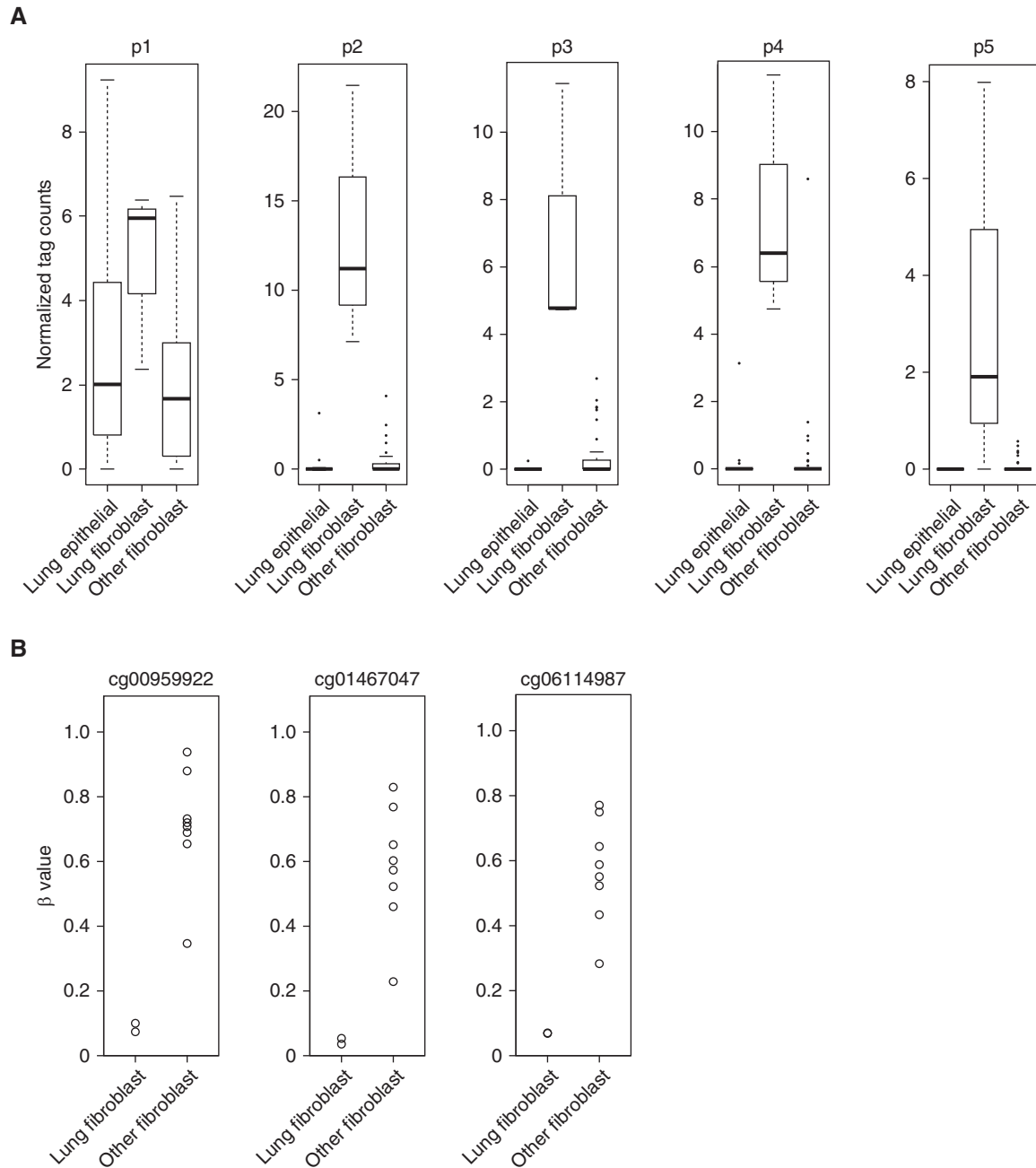


**Figure 1.** Higher expression of *FOXL1* (forkhead box L1) in lung fibroblasts. (A) Box plot showing normalized cap analysis of gene expression (CAGE) tag counts of p1, p2, p3, p4, and p5 promoters annotated to *FOXL1*. CAGE data were compared among the following three groups: 16 lung epithelial cell lines (alveolar, small airway, bronchial, and tracheal epithelial cells), three lung fibroblast lines, and 42 other fibroblast lines that included gingival fibroblasts ( $n = 6$ ), periodontal ligament fibroblasts ( $n = 6$ ), cardiac fibroblasts ( $n = 6$ ), choroid plexus fibroblasts ( $n = 3$ ), conjunctival fibroblasts ( $n = 2$ ), dermal fibroblasts ( $n = 6$ ), aortic adventitial fibroblasts ( $n = 3$ ), lymphatic fibroblasts ( $n = 3$ ), mammary fibroblasts ( $n = 3$ ), pulmonary artery fibroblast ( $n = 1$ ), and villous mesenchymal fibroblasts ( $n = 3$ ). The central line in the box indicates the median value. (B) DNA methylation levels shown as  $\beta$  values (the GSE40699 dataset) were compared between lung fibroblast lines ( $n = 2$ ) and other fibroblast lines ( $n = 8$ ). CpG sites located upstream from the transcription start site (TSS) are indicated (cg00959922, cg01467047, and cg06114987).

approved by the Ethics Committee at the National Hospital Organization Tokyo National Hospital Institutional Review Board (5). Antigen retrieval was

accomplished in citrate buffer (pH of 6.0 at 98°C for 40 min). Anti-FOXL1 rabbit polyclonal antibody (ab190226; Abcam) or anti-vimentin (V9) mouse monoclonal

antibody (IR630; Dako) was used. Tissue sections were processed with the Vectastain Elite ABC Kit (Vector Laboratories).

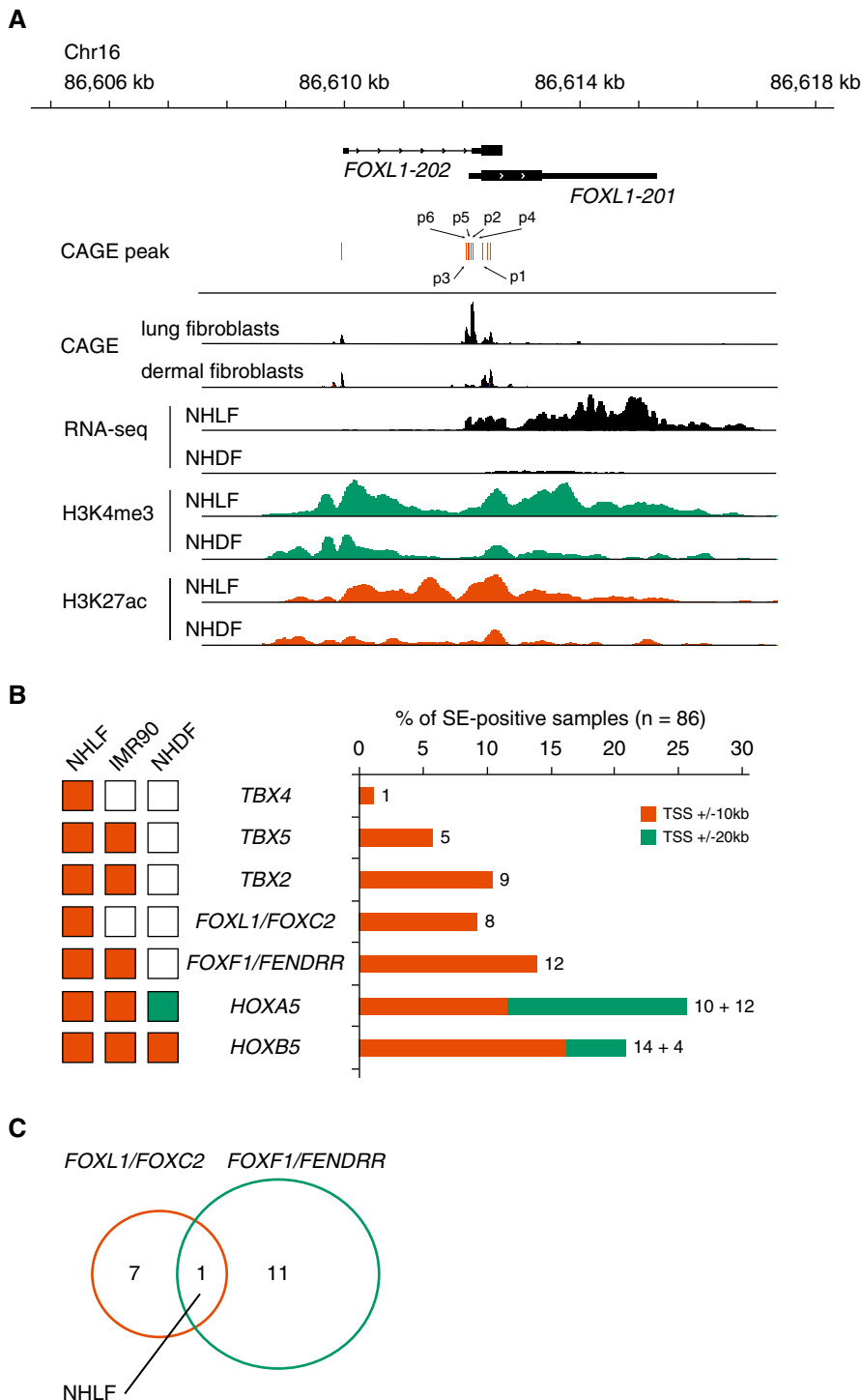


**Figure 2.** *FOXL1* is associated with super-enhancers in lung fibroblasts. (A) Genomic coordinates, *FOXL1* transcripts, and CAGE peaks are indicated. CAGE-sequencing data were merged from three lung fibroblast lines or six dermal fibroblast lines. RNA-sequencing (RNA-seq) signals and ChIP (chromatin immunoprecipitation) peaks of H3K4me3 and H3K27ac in normal human lung fibroblasts (NHLF) or normal human dermal fibroblasts (NHDF) are shown. Note that CAGE peaks, RNA-seq signals, and active histone marks (H3K4me3 and H3K27ac) for *FOXL1* are more apparent in lung fibroblasts than in dermal fibroblasts. The same y-axis scales are used for the comparisons between NHLF and NHDF. (B) Left: associations of transcription factors with super-enhancers among NHLF, IMR90, and NHDF. Super-enhancers were identified as reported previously (8).

### RNA *in Situ* Hybridization

RNA *in situ* hybridization (ISH) was performed on human lung tissue sections obtained from three transplant donors (Table E4) who were previously healthy, as described previously (31). The protocol to procure human lung tissue was approved by the University of North Carolina Institutional Review Board (03-1396). The probes and reagents were used according to the RNAscope protocol from Advanced Cell Diagnostics.

### Statistical Analysis

Differences were examined by Dunnett test with JMP version 13 (SAS Institute Inc.). Pearson's correlation coefficient ( $r$ ) and decision coefficient ( $R^2$ ) were calculated for correlation analysis.

## Results

### Higher Expression of *FOXL1* Transcripts in Lung Fibroblasts

Human fibroblasts isolated from different anatomical sites are heterogeneous in terms of their gene expression patterns (3). To obtain a gene list that defines the pulmonary origin of lung fibroblasts, we used the Cap Analysis of Gene Expression (CAGE) dataset from the FANTOM5 (Functional ANnotation Of the Mammalian genome 5) consortium (32) and analyzed transcriptome data from 45 different fibroblast lines (5) in search of CAGE-defined transcription start sites (also termed "promoters" in the FANTOM5 project) that are selectively activated in lung fibroblasts. By comparing the CAGE profiles among three human lung-derived fibroblast lines and 42 other fibroblast lines, we identified 189 promoters (including those of 88 protein-coding genes) with lung-specific expression (5). Among these, 37 promoters were annotated to transcription factors; *TBX4*, *TBX5*, *FOXL1*, *HOXA5*, and *HOXB5* were among the top 10 promoters ranked by false discovery rate (Table E5).

We recently explored the functional roles of *TBX4* and other T-box family genes (*TBX2* and *TBX5*) in lung fibroblasts (5). The crucial importance of Hox5 genes (including *Hoxa5* and *Hoxb5*) in lung morphogenesis and in lung fibroblast function has also been described (33). However, no reports have described the role of *FOXL1* in the lungs or lung

fibroblasts; thus, we selected the *FOXL1* gene for further analysis.

There are two transcripts of human *FOXL1* (designated *FOXL1-201* and *FOXL1-202*); the major transcript (*FOXL1-201*), encoding full-length *FOXL1*, is composed of a single exon with multiple transcription start sites. In the analyzed CAGE dataset, alternative promoters for the same gene are ranked by their expression levels and numbered (e.g., p1, p2, and p3) (32). Four different promoters annotated to *FOXL1-201* (p2, p3, p4, and p5) were included in the above-mentioned 189 promoters. To ascertain the specific activity of *FOXL1* promoters in lung fibroblasts, we compared CAGE count data among three groups, including 16 lung epithelial cell lines, three lung fibroblast lines, and 42 other fibroblast lines. We confirmed that *FOXL1* expression from p2, p3, p4, and p5 promoters was prominent in lung fibroblast lines, and p2 promoter-derived transcripts were the most abundant. On the other hand, p1 promoter showed activation in all three groups (Figure 1A). Thus, the major transcription start site for *FOXL1* in lung fibroblasts (p2 promoter) was distinct from that in other cell types (p1 promoter).

We next compared DNA methylation levels ( $\beta$  values) of the *FOXL1* gene between two human lung fibroblast lines and eight other fibroblast lines using the GSE40699 dataset (Infinium 450K methylation array) from the ENCODE (Encyclopedia of DNA Elements) project (34, 35). In agreement with the finding of higher *FOXL1* expression in lung fibroblasts, most of the 11 methylation probes annotated to *FOXL1* showed lower  $\beta$  values in lung fibroblast lines than in other fibroblast lines. Of particular note, CpG sites located in the promoter region upstream from the transcription start site (cg00959922, cg01467047, and cg06114987) were evidently hypomethylated in lung fibroblast lines in clear contrast to other fibroblast lines (Figure 1B).

### **FOXL1 Is Associated with Super-Enhancers in Lung Fibroblasts**

To investigate the epigenetic regulation of *FOXL1*, we compared expression levels (RNA-seq) and histone H3 modifications between normal human lung fibroblasts NHLF (normal human lung fibroblasts) and NHDF (normal human dermal fibroblasts) using the ENCODE datasets (34, 35). Consistent with our observations from the CAGE dataset, *FOXL1* transcripts were higher in NHLF, and the *FOXL1* locus was enriched in active histone marks, histone H3 acetylation at lysine 27 (H3K27ac), and H3 methylation at lysine 4 (H3K4me3) (Figure 2A).

Super-enhancers are large genomic regions defined by exceptional enrichment of Mediator complexes and master transcription factors or by high concentrations of H3K27ac that induce the expression of cell identity genes (6–8). We explored the presence of super-enhancers at *TBX2*, *TBX4*, *TBX5*, *HOXA5*, *HOXB5*, *FOXL1/FOXC2*, and *FOXF1/FENDRR* gene loci across 86 human cell line and tissue samples that included IMR90 (human fetal lung fibroblasts), NHLF, and NHDF (Table E6). *FOXL1/FOXC2* genes were found to be associated with super-enhancers in eight samples, including NHLF, human umbilical vein endothelial cells, astrocytes, and osteoblasts (Figure 2B). Notably, among 86 samples, both *FOXL1/FOXC2* and *FOXF1/FENDRR* were associated with super-enhancers only in NHLF, suggesting that a highly activated FOX gene cluster is a hallmark of lung fibroblasts (Figure 2C). Visualization of H3K27ac ChIP-seq signals in different cell line and tissue samples showed that broad peaks in both *FOXL1/FOXC2* and *FOXF1/FENDRR* gene loci were characteristic of lung fibroblasts (NHLF and IMR90) and appeared associated with cellular identity (see Figure E1 in the data supplement).

We also reanalyzed a recently reported single-cell RNA-seq dataset of mouse lung mesenchymal cells (17) (Figure E2A) and found that *Foxl1* was preferentially expressed in the *Axin2*<sup>+</sup>*Pdgfra*<sup>+</sup> mesenchymal

cell subpopulation that was reportedly involved in lung regeneration (Figure E2B). These observations suggested that *FOXL1* might have important roles both in human lung fibroblasts and in mouse lung mesenchymal cells.

### **Expression of FOXL1 in Human Lung Tissue**

To characterize topographic distribution of *FOXL1* expression in the lungs, we performed RNA ISH and immunohistochemistry. *FOXL1* mRNA (Figures 3A and E3) and protein (Figure 3B) showed concordant expression patterns throughout the airway, and nuclear positivity for *FOXL1* was detected in the airway epithelium. *FOXL1*-positive cells were also found in the submucosal interstitium, where fibroblasts reside. Positive staining of *FOXL1* in interstitial cells was commonly observed among the analyzed lung specimens. *FOXL1* expression was also observed in the nuclei of alveolar cells by both RNA ISH (Figure 3A) and immunohistochemistry (Figure 3B), although it was hard to identify each cell type. Importantly, immunohistochemical studies indicated that *FOXL1*-positive interstitial cells were also stained for vimentin (Figure 3B), suggesting the presence of resident fibroblasts expressing *FOXL1*.

### **RNA-Seq Analysis of Lung Fibroblasts after FOXL1 Knockdown**

To identify genes possibly regulated by *FOXL1*, we performed an RNA-seq analysis of NHLF treated with *FOXL1* siRNA (si*FOXL1*). Using a threshold of reads per kilobase of transcript per million mapped reads of greater than one in negative control siRNA (siNC)-treated cells and a log<sub>2</sub> fold change of less than -0.5 both in the si*FOXL1* groups 1 and 2, we found 273 downregulated transcripts after *FOXL1* knockdown (Table E7). These transcripts defined a si*FOXL1*-downregulated gene signature, which was used for further analysis.

Gene ontology analysis showed that the si*FOXL1*-downregulated gene signature was enriched with genes involved in inflammatory response, cell–cell signaling, and regulation of cell growth, suggesting

**Figure 2.** (Continued). Right: associations of transcription factors with super-enhancers among 86 human cell line and tissue samples. Super-enhancers overlapping with  $\pm 10$  or 20 kb from the TSSs of the indicated genes were identified. Numbers of samples positive for super-enhancers are indicated. (C) Venn diagram showing that NHLF is the only sample in which both *FOXL1/FOXC2* and *FOXF1/FENDRR* are associated with super-enhancers. Chr = chromosome; FENDRR = *FOXF1* adjacent non-coding developmental regulatory RNA; *HOXA5* = homeobox A5; SE-positive = super-enhancer-positive; *TBX4* = T-box transcription factor 4.

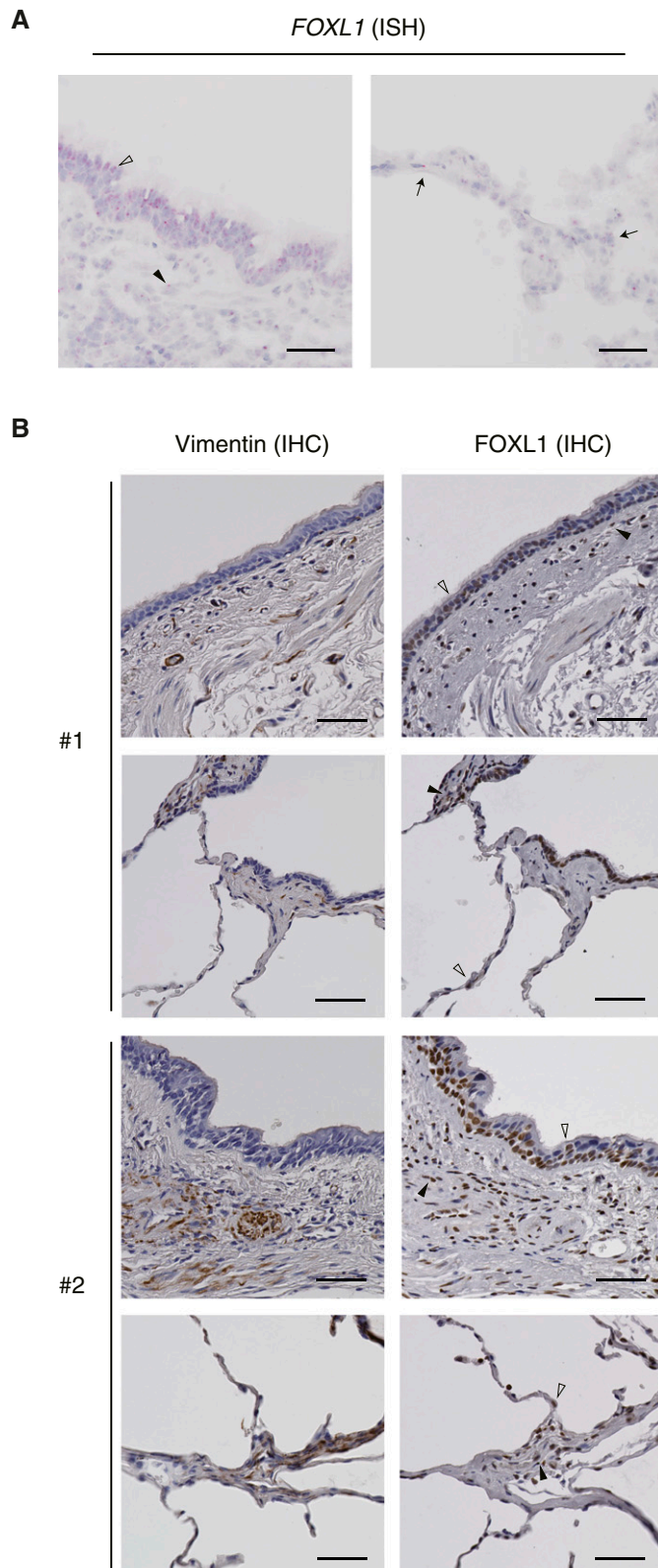


**Figure 3.** Expression of *FOXL1* in human lung tissue. (A) *FOXL1* expression detected by RNA ISH in normal lung tissue. Left: *FOXL1* was positively stained in the nuclei of both epithelial cells (open arrowhead) and interstitial cells (solid arrowhead) in the airway. Right: Nuclear *FOXL1* positivity was found in the alveolar cells (arrows). Scale bars, 50  $\mu\text{m}$ . (B) Immunohistochemistry (IHC) for vimentin

that *FOXL1* is involved in various fibroblast functions (Figure 4A and Table E8).

### ***FOXL1* Is Related to TAZ/YAP Signaling in Lung Fibroblasts**

Next, we performed gene set enrichment analysis using different gene signatures derived from the C6 oncogenic signature collection of the Molecular Signatures Database (version 7.0). Among them, “YAP-conserved signature” (70 genes) showed a high association with the genes downregulated by *FOXL1* knockdown (Figure 4B). In line with this finding, motif analysis of the promoter regions of the si*FOXL1*-downregulated gene signature revealed that TEAD-binding consensus sequences were enriched, together with those for FOX genes (Figure E4). In our previous study, we defined “TAZ-regulated signature” (94 genes) in lung fibroblasts (25). Gene set enrichment analysis indicated that TAZ-regulated signature and YAP-conserved signature were enriched among the genes downregulated by *FOXL1* knockdown in lung fibroblasts (25, 27, 36) (Figure 4C).

A comparison between the si*FOXL1*-downregulated gene signature (273 genes) and TAZ-regulated signature (25) revealed 12 common genes, including *CTGF*, *GREM1* (gremlin 1), and *FSTL1* (follistatin-like 1). For further validation, we performed IB for *CTGF* in lung fibroblasts treated with siNC or si*FOXL1* and confirmed its decreased expression at the protein level after *FOXL1* silencing (Figure 4D).

### ***FOXL1* Is Related to BMP Signaling in Lung Fibroblasts**

Recent studies indicated that BMP signaling has a substantial impact on epithelial–mesenchymal interactions and is important for murine lung homeostasis (37, 38). As noted above, BMP signaling antagonists (*GREM1* and *FSTL1*) were downregulated by *FOXL1* knockdown (38). In addition, we found that the expression of BMP ligands (*BMP2* and *BMP4*) was also decreased after *FOXL1* knockdown (Table E7).

To further explore the relationships between *FOXL1* and BMP ligands/antagonists (*BMP2*, *BMP4*, *GREM1*, and *FSTL1*), we compared their expression levels by quantitative RT-PCR in 17

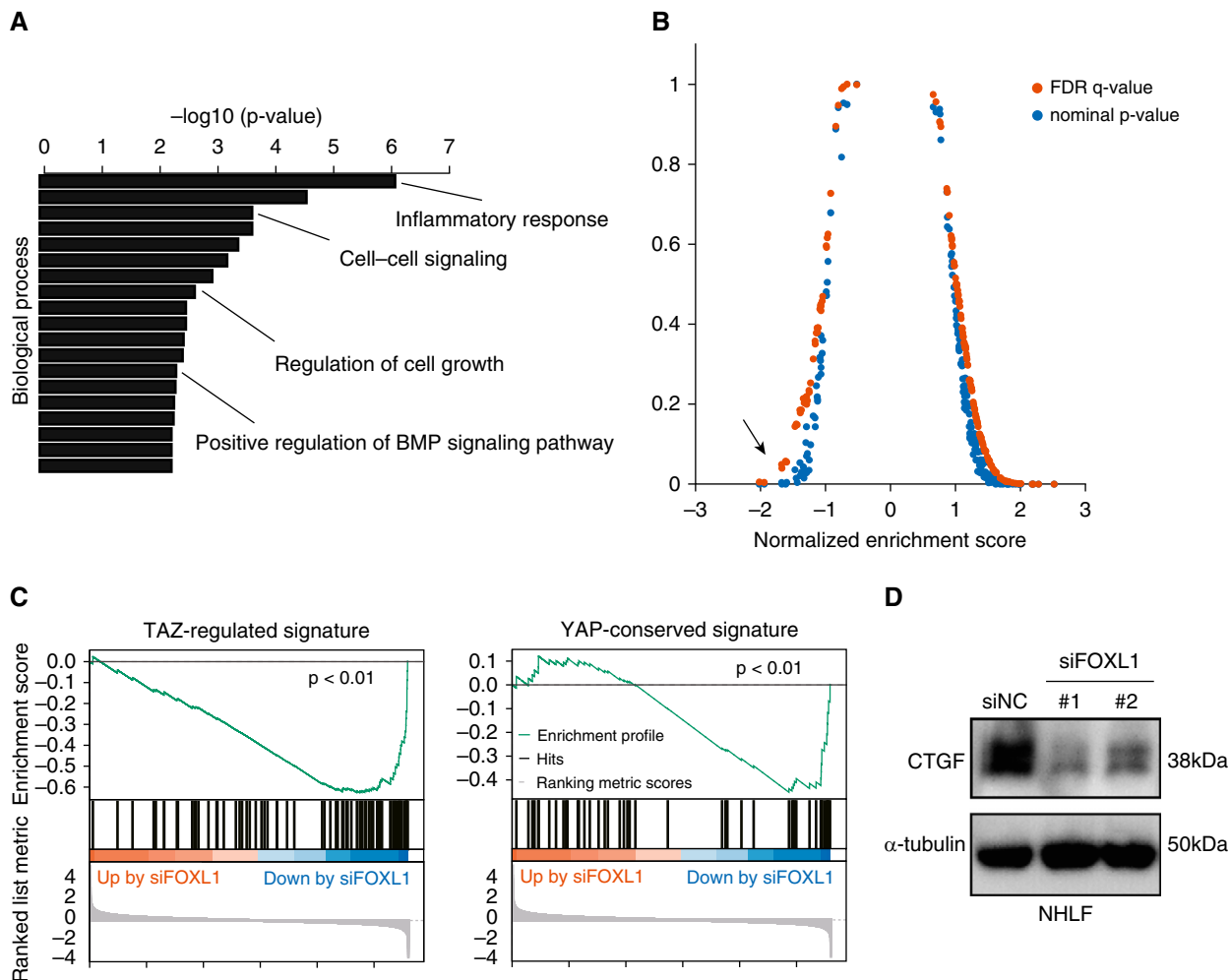


**Figure 4.** RNA-seq analysis of lung fibroblasts after *FOXL1* knockdown. (A) Gene ontology analysis was performed using the *FOXL1* siRNA (siFOX1)-downregulated gene signature (273 genes). Enriched gene ontology terms for biological process are sorted by  $-\log_{10}(P)$  value. (B) Gene set enrichment analysis was performed using the RNA-seq result and different gene signatures derived from the C6 oncogenic signature collection of the Molecular Signatures Database. YAP (Yes-associated protein)-conserved signature indicated by the arrow showed a high association with the genes downregulated by *FOXL1* knockdown. (C) Gene set enrichment analysis was performed using the RNA-seq data in NHLF with *FOXL1* knockdown using TAZ (transcriptional coactivator with PDZ-binding motif)-regulated signature defined by our previous study (left) or YAP-conserved signature from the Molecular Signatures Database (right). (D) IB for CTGF (connective tissue growth factor) in NHLF treated with negative control siRNA (siNC) or siFOX1 (#1 or #2).  $\alpha$ -tubulin was used as the loading control. BMP = bone morphogenetic protein; FDR = false discovery rate.

different human lung fibroblast lines (Table E2). In line with our RNA-seq result, *FOXL1* expression levels were positively correlated with *BMP2* ( $r = 0.91$ ), *BMP4* ( $r = 0.72$ ), and *GREM1* ( $r = 0.54$ ), suggesting that *FOXL1* positively regulates BMP ligands and antagonists, and thereby tunes BMP signaling (Figures 5A and E5A).

Next, we explored the functional relevance of *FOXL1* in association with BMP signaling in lung fibroblasts.

*BMP4* treatment enhanced cell growth in NHLF (Figure 5B). On the other hand, *FOXL1* knockdown tended to suppress cell growth (Figure 5B). Three-dimensional collagen gels embedded with fibroblasts are used as a model of fibroblast-mediated tissue contraction (30). Exogenous *BMP4* promoted contraction of collagen gels embedded with NHLF, whereas *FOXL1* knockdown inhibited collagen gel contraction (Figure 5C).

### FOXL1 Is Related to PDGF Signaling in Lung Fibroblasts

PDGF signaling in the mesenchyme is essential for lung morphogenesis (16) and *Pdgfra*<sup>+</sup> lung fibroblasts contribute to lung regeneration in mice (15, 39). We noted that *PDGFRA* was downregulated by *FOXL1* knockdown in our RNA-seq dataset (Table E7), and this effect was further confirmed at the protein level in two different lung fibroblast lines, NHLF and HFL1 (human fetal lung fibroblasts)

**Figure 3.** (Continued). (left) and *FOXL1* (right) in normal lung tissue. Two different subjects (#1 and #2) are presented. *FOXL1* was positively stained in the nuclei of both epithelial cells (open arrowheads) and interstitial cells (solid arrowheads) in the airway (top) and the alveolus (bottom). Note that nuclear *FOXL1* staining is observed in the interstitial cells positive for vimentin. Scale bars, 50  $\mu$ m. ISH = *in situ* hybridization.

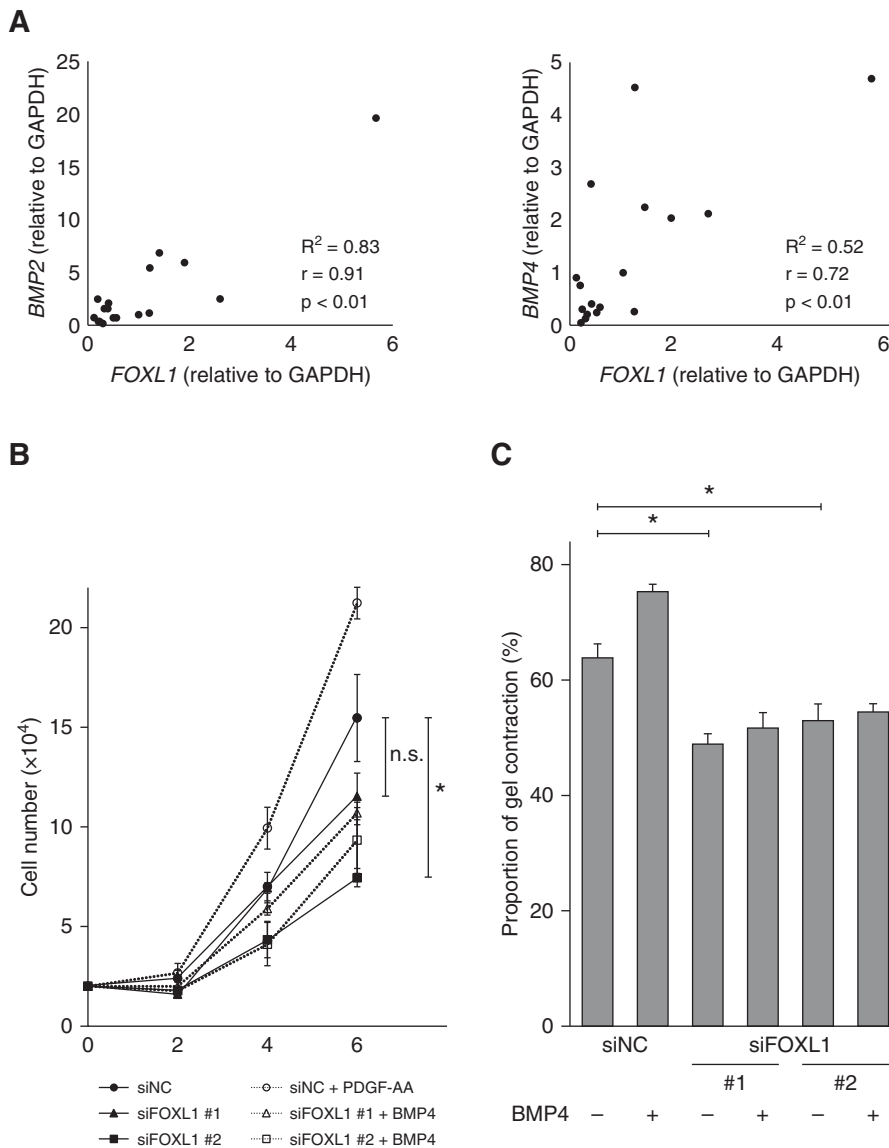


**Figure 5.** *FOXL1* is related to BMP signaling in lung fibroblasts. (A) Associations of expression levels between *FOXL1* and BMP ligands (*BMP2* and *BMP4*) in lung fibroblast lines ( $n = 17$ ) were evaluated by quantitative RT-PCR. The expression levels were normalized to that of *GAPDH*. (B) Cell numbers of NHLF transfected with siNC or siFOXL1 (#1 or #2) in the presence or absence of BMP4 (20 ng/ml) were counted 2, 4, and 6 days after seeding. The experiments were performed in triplicate. Error bars represent SEs. The cells transfected with siFOXL1 (#1 or #2) were compared with the siNC-transfected cells in the absence of BMP4. \* $P < 0.05$ . (C) NHLF transfected with siNC or siFOXL1 (#1 or #2) in the presence or absence of BMP4 (20 ng/ml) were embedded in collagen gels ( $n = 6$ ). After 72 hours, the area of each gel was quantified. The percentage of contracted gel area was measured and compared with the initial size. Error bars represent SEs. The cells transfected with siFOXL1 (#1 or #2) were compared with the siNC-transfected cells in the absence of BMP4. \* $P < 0.05$ . n.s. = not significant.

(Figure 6A). This observation suggested that *FOXL1* could regulate lung fibroblast functions by modulating PDGF signaling (40).

We tested whether *FOXL1* silencing could affect cell growth in the presence or absence of PDGF-AA stimulation.

PDGF-AA tended to promote cell growth of both NHLF and HFL1, whereas *FOXL1* knockdown suppressed it (Figure 6B). Similarly, PDGF-AA tended to enhance collagen gel contraction in both fibroblast lines, whereas *FOXL1* knockdown inhibited it (Figure 6C). In addition, *FOXL1*

knockdown inhibited the migration of NHLF (Figure E6).

PDGF-AA can only activate PDGFR $\alpha$  homodimers, not PDGFR $\alpha$ /PDGFR $\beta$  heterodimers or PDGFR $\beta$  homodimers (41). Given that *FOXL1* knockdown leads to PDGFR $\alpha$  downregulation (Figure 6A), the effects of *FOXL1* knockdown could be partly attributed to attenuated PDGF signaling.

Collectively, our results showed that *FOXL1* governs a subset of genes related to key signaling (*CTGF*, *PDGFRA*, *BMP2*, and *BMP4*) in lung fibroblasts. We further explored *FOXL1* and *TEAD4* binding sequences (Figure E7A) in the promoter regions of these genes and identified multiple putative recognition sites (Figure E7B). These observations suggested that these genes could be partly regulated in a direct manner by *FOXL1* or *TAZ/YAP* signaling.

### **FOXL1 Is Expressed in Fibroblasts of IPF Lung Tissue**

It is widely accepted that fibroblasts are key effector cells responsible for tissue fibrosis. Clusters of fibroblasts distributed in IPF lung tissue are presumed to be the sites of fibrotic reaction (23). To explore the clinical significance of *FOXL1* expression in the lungs, we compared the transcript levels of *FOXL1* between normal and IPF lung tissues using the GSE92592 dataset (42) and found higher *FOXL1* expression levels in IPF lung tissue (Figure 7A).

Previous studies demonstrated that *GREM1* and *FSTL1* are increased in IPF lung tissue and are involved in IPF pathogenesis (43, 44). Because fibroblasts are the major source of these molecules, we compared the transcript levels of *FOXL1* with those of *GREM1* and *FSTL1* in normal and IPF lung tissues. In agreement with the previous reports (43, 44), *GREM1* and *FSTL1* expression levels were higher in IPF lung tissue (Figure E5B). Moreover, they showed positive correlations with *FOXL1* ( $r = 0.54$  for *GREM1* and  $r = 0.69$  for *FSTL1*), supporting the notion that *GREM1* and *FSTL1* are positively regulated by *FOXL1* (Table E7 and Figure E5A). These observations also suggested that *FOXL1* might be functionally active to regulate a subset of target genes in IPF lung tissue.

We further compared *FOXL1* expression levels in lung fibroblasts



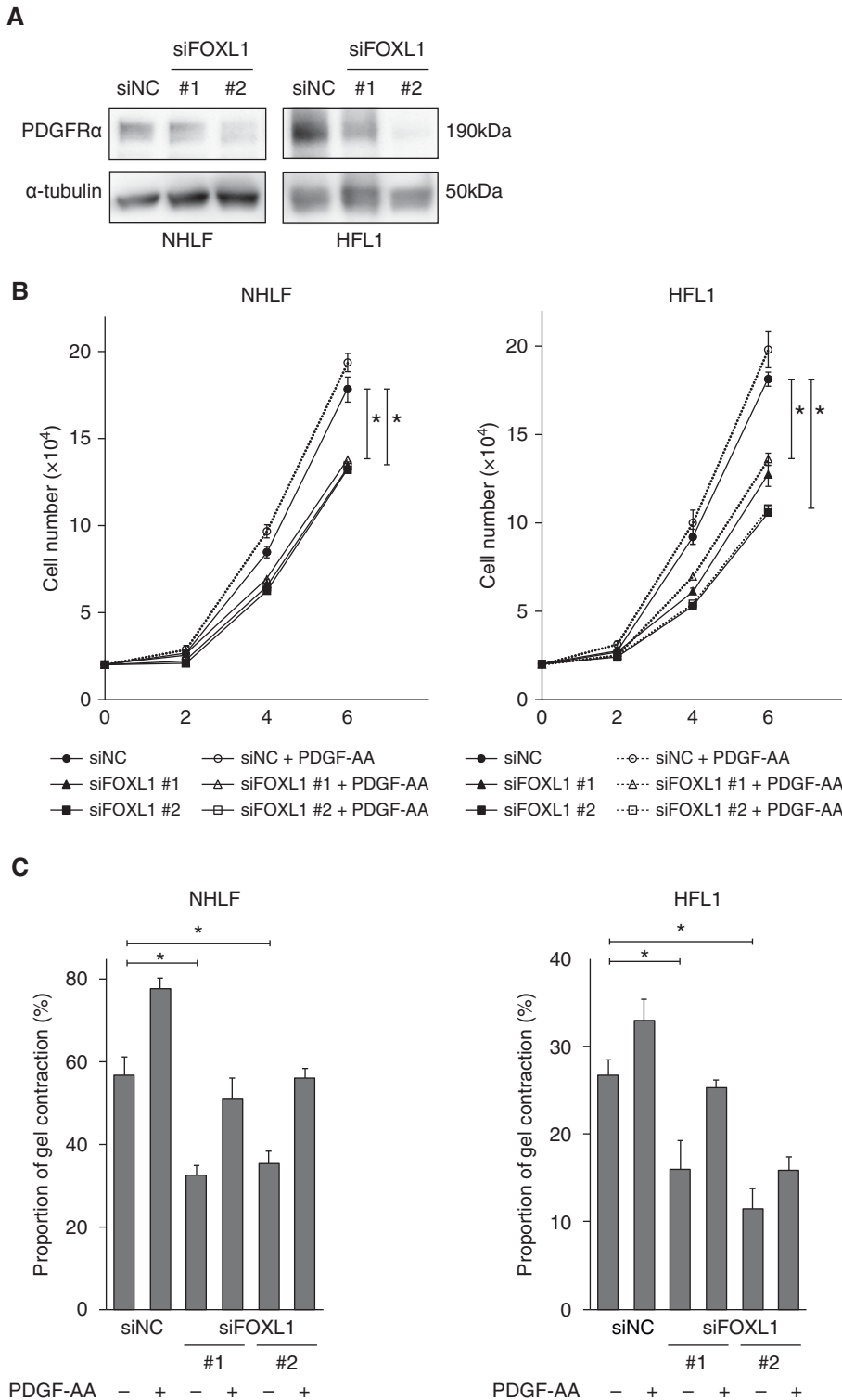


**Figure 6.** *FOXL1* is related to PDGF (platelet-derived growth factor) signaling in lung fibroblasts. (A) IB for PDGFR $\alpha$  (PDGF receptor- $\alpha$ ) in NHLF and HFL1 treated with siNC or siFOXL1 (#1 or #2).  $\alpha$ -tubulin was used as the loading control. (B) Cell numbers of NHLF or HFL1 (human fetal lung fibroblasts) transfected with siNC or siFOXL1 (#1 or #2) in the presence or absence of PDGF-AA (10 ng/ml) were counted 2, 4, and 6 days after seeding. The experiments were performed in quadruplicate. Error bars represent SEs. The cells transfected with siFOXL1 (#1 or #2) were compared with the siNC-transfected cells in the absence of PDGF-AA. \* $P < 0.05$ . (C) NHLF or

derived from normal and IPF lung tissues. Consistent with the results in lung tissue samples, *FOXL1* expression was increased in lung fibroblasts derived from IPF lung tissue at the transcript level (Figure 7B).

Finally, we investigated *FOXL1* protein expression in IPF lung tissue and found *FOXL1* immunoreactivity in the nuclei of fibroblasts, which were also positive for vimentin (Figure 7C). Positive staining of *FOXL1* in fibroblasts was commonly observed among the lung specimens derived from three different patients with IPF, suggesting its role in IPF pathogenesis.

## Discussion

Fibroblasts are heterogeneous populations, and previous transcriptome analyses have demonstrated organ-specific gene signatures that represent “positional memory” of cultured fibroblasts. In search of a lung-specific fibroblast signature, our unbiased screening using the FANTOM5 database, including 45 different fibroblast lines, identified *FOXL1* as a transcription factor highly activated in fibroblasts derived from the lungs. This was further supported by the findings based on the ENCODE database that the *FOXL1* gene in lung fibroblasts is selectively hypomethylated and associated with super-enhancers.

Recent studies demonstrated that *Foxl1*-positive mesenchymal cells in the murine intestine, which are also positive for *Pdgfra*, are crucial for the intestinal stem cell niche (12, 13). It is also suggested that mesenchymal cells marked by *Foxl1* and *Pdgfra* expression are so-called “telocytes” (45–47), which constitute a morphologically defined cell type found in various organs, including the lungs (48). It is known that *Pdgfra*<sup>+</sup> alveolar fibroblasts contribute to alveolar epithelial self-renewal in mice (15, 17), and it was noteworthy that *Foxl1* expression was found in *Pdgfra*<sup>+</sup> murine lung mesenchymal cells by reanalysis of single-cell RNA-seq data (Figure E2B) (17).

It should be noted that the 45 fibroblast lines analyzed in this study do not include fibroblasts of gut origin. Considering that both the lungs and the gastrointestinal tract are endoderm-derived organs, it would be interesting to identify similarities and

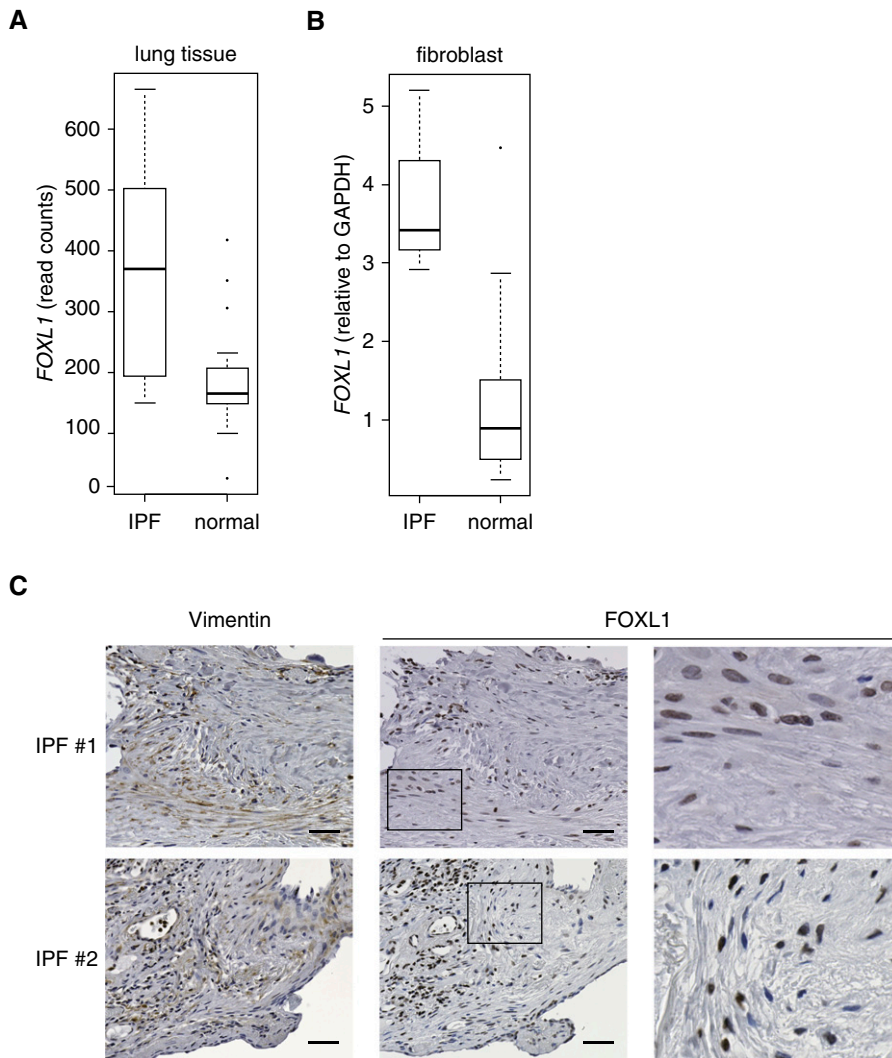


**Figure 7.** *FOXL1* is expressed in the fibroblasts of idiopathic pulmonary fibrosis (IPF) lung tissue. (A) Transcript levels of *FOXL1* in normal ( $n = 19$ ) and IPF ( $n = 20$ ) lung tissues. RNA-seq data were obtained from the GSE92592 dataset. (B) Transcript levels of *FOXL1* in lung fibroblast lines derived from normal subjects ( $n = 14$ ) and lung fibroblast lines derived from patients with IPF ( $n = 3$ ). Quantitative RT-PCR was performed, and relative expression levels were normalized to those of *GAPDH*. (C) IHC for vimentin and *FOXL1* in IPF lung tissue. Two different IPF cases are presented. High-magnification views of rectangular area of *FOXL1* immunostaining are shown to the right. Note that nuclear *FOXL1* staining is observed in the fibroblasts positive for vimentin. Scale bars, 50  $\mu\text{m}$ .

differences between lung fibroblasts and gastrointestinal fibroblasts.

In the present study, we explored genes possibly regulated by *FOXL1* and investigated functional roles of *FOXL1* in cultured human lung fibroblasts. Our RNA-seq analysis suggested that

*FOXL1* modulates key signaling pathways, including CTGF, BMP, and PDGF, through transcriptional regulation of their ligands, antagonists, or receptors. Moreover, cell culture studies revealed that *FOXL1* could regulate key cellular responses such as

cell growth and collagen gel contraction, all of which are important for the processes of wound healing and fibrogenesis.

Recent evidence suggests that fibroblast- or mesenchyme-derived Wnt and BMP signals are crucial for alveolar epithelial cell proliferation and differentiation (38, 49). Although we did not find a clear decrease in Wnt ligands after *FOXL1* knockdown, our results indicate that *FOXL1* could positively regulate BMP ligands (*BMP2* and *BMP4*) and antagonists (*GREM1* and *FSTL1*). Indeed, quantitative RT-PCR experiments showed positive correlations of expression levels between *FOXL1* and these BMP ligands/antagonists (38). *FOXL1*-mediated modulation of BMP signaling and its pathophysiological role in the context of epithelial-mesenchymal interactions are worthy of further investigation.

In IPF lung tissue, pathologically activated lung fibroblasts are responsible for excessive ECM deposition and fibrotic responses (22). Furthermore, alveolar epithelial cell proliferation and differentiation are dysregulated in IPF lung tissue (50) at least partly because of the influence of activated fibroblasts. Taken together with our finding that *FOXL1* is expressed in fibroblasts of IPF lung tissue, *FOXL1* may be an important player in the pathological processes of IPF. ■

**Author disclosures** are available with the text of this article at [www.atsjournals.org](http://www.atsjournals.org).

**Acknowledgment:** The authors thank Sayaka Arakawa and Sayaka Igarashi for their assistance for primary cultured lung fibroblasts obtained at Tokyo National Hospital. They also thank Isao Asari for his excellent technical assistance with immunohistochemistry. Human lung specimens were provided by the University of North Carolina Marsico Lung Institute Tissue Procurement and Cell Culture Core, which is supported in part by the Cystic Fibrosis Foundation (grant BOUCHE19R0) and the National Institutes of Health (grant DK065988). The authors also thank Rodney C. Gilmore for performing RNA ISH. They also thank the members of the Department of Respiratory Medicine of the Graduate School of Medicine at the University of Tokyo for their support and useful discussion.

**Figure 6.** (Continued). HFL1 transfected with siNC or si*FOXL1* (#1 or #2) in the presence or absence of PDGF-AA (10 ng/ml) were embedded in collagen gels. After 72 hours, the area of each gel was quantified. Percentage of contracted gel area was measured and compared with the initial size. The experiments were performed in triplicate. Error bars represent SEs. The cells transfected with si*FOXL1* (#1 or #2) were compared with the siNC-transfected cells in the absence of PDGF-AA. \* $P < 0.05$ .

## References

- Micke P, Ostman A. Tumour-stroma interaction: cancer-associated fibroblasts as novel targets in anti-cancer therapy? *Lung Cancer* 2004; 45:S163–S175.
- Peyser R, MacDonnell S, Gao Y, Cheng L, Kim Y, Kaplan T, et al. Defining the activated fibroblast population in lung fibrosis using single-cell sequencing. *Am J Respir Cell Mol Biol* 2019;61: 74–85.
- Chang HY, Chi JT, Dudoit S, Bondre C, van de Rijn M, Botstein D, et al. Diversity, topographic differentiation, and positional memory in human fibroblasts. *Proc Natl Acad Sci USA* 2002;99: 12877–12882.
- Horie M, Yamaguchi Y, Saito A, Nagase T, Lizio M, Itoh M, et al. Transcriptome analysis of periodontitis-associated fibroblasts by CAGE sequencing identified DLX5 and RUNX2 long variant as novel regulators involved in periodontitis. *Sci Rep* 2016;6: 33666.
- Horie M, Miyashita N, Mikami Y, Noguchi S, Yamauchi Y, Suzukawa M, et al. TBX4 is involved in the super-enhancer-driven transcriptional programs underlying features specific to lung fibroblasts. *Am J Physiol Lung Cell Mol Physiol* 2018;314:L177–L191.
- Suzuki HI, Young RA, Sharp PA. Super-enhancer-mediated RNA processing revealed by integrative microRNA network analysis. *Cell* 2017;168:1000–1014, e15.
- Whyte WA, Orlando DA, Hnisz D, Abraham BJ, Lin CY, Kagey MH, et al. Master transcription factors and mediator establish super-enhancers at key cell identity genes. *Cell* 2013;153:307–319.
- Hnisz D, Abraham BJ, Lee TI, Lau A, Saint-André V, Sigova AA, et al. Super-enhancers in the control of cell identity and disease. *Cell* 2013; 155:934–947.
- Lehmann OJ, Sowden JC, Carlsson P, Jordan T, Bhattacharya SS. Fox's in development and disease. *Trends Genet* 2003;19:339–344.
- Kaestner KH, Bleckmann SC, Monaghan AP, Schlöndorff J, Mincheva A, Lichter P, et al. Clustered arrangement of winged helix genes fkh-6 and MFH-1: possible implications for mesoderm development. *Development* 1996;122:1751–1758.
- Kaestner KH, Silberg DG, Traber PG, Schütz G. The mesenchymal winged helix transcription factor Fkh6 is required for the control of gastrointestinal proliferation and differentiation. *Genes Dev* 1997;11: 1583–1595.
- Aoki R, Shoshkes-Carmel M, Gao N, Shin S, May CL, Golson ML, et al. FoxI1-expressing mesenchymal cells constitute the intestinal stem cell niche. *Cell Mol Gastroenterol Hepatol* 2016;2: 175–188.
- Shoshkes-Carmel M, Wang YJ, Wangenstein KJ, Tóth B, Kondo A, Massasa EE, et al. Subepithelial telocytes are an important source of Wnts that supports intestinal crypts. *Nature* 2018;557: 242–246.
- Uhlén M, Fagerberg L, Hallström BM, Lindskog C, Oksvold P, Mardinoglu A, et al. Proteomics: tissue-based map of the human proteome. *Science* 2015;347:1260419.
- Barkauskas CE, Crouse MJ, Rackley CR, Bowie EJ, Keene DR, Stripp BR, et al. Type 2 alveolar cells are stem cells in adult lung. *J Clin Invest* 2013;123:3025–3036.
- Boström H, Grittli-Linde A, Betsholtz C. PDGF-A/PDGF alpha-receptor signaling is required for lung growth and the formation of alveoli but not for early lung branching morphogenesis. *Dev Dyn* 2002;223: 155–162.
- Zepp JA, Zacharias WJ, Frank DB, Cavanaugh CA, Zhou S, Morley MP, et al. Distinct mesenchymal lineages and niches promote epithelial self-renewal and myofibrogenesis in the lung. *Cell* 2017;170: 1134–1148, e10.
- Kulkarni T, O'Reilly P, Antony VB, Gaggar A, Thannickal VJ. Matrix remodeling in pulmonary fibrosis and emphysema. *Am J Respir Cell Mol Biol* 2016;54:751–760.
- Sanders YY, Liu H, Scruggs AM, Duncan SR, Huang SK, Thannickal VJ. Epigenetic regulation of caveolin-1 gene expression in lung fibroblasts. *Am J Respir Cell Mol Biol* 2017;56:50–61.
- Kato K, Logsdon NJ, Shin YJ, Palumbo S, Knox A, Irish JD, et al. Impaired myofibroblast dedifferentiation contributes to nonresolving fibrosis in aging. *Am J Respir Cell Mol Biol* 2020;62:633–644.
- Richeldi L, Collard HR, Jones MG. Idiopathic pulmonary fibrosis. *Lancet* 2017;389:1941–1952.
- Thannickal VJ, Zhou Y, Gaggar A, Duncan SR. Fibrosis: ultimate and proximate causes. *J Clin Invest* 2014;124:4673–4677.
- Hinz B, Phan SH, Thannickal VJ, Prunotto M, Desmoulière A, Varga J, et al. Recent developments in myofibroblast biology: paradigms for connective tissue remodeling. *Am J Pathol* 2012;180: 1340–1355.
- Saito A, Nagase T. Hippo and TGF- $\beta$  interplay in the lung field. *Am J Physiol Lung Cell Mol Physiol* 2015;309:L756–L767.
- Noguchi S, Saito A, Mikami Y, Urushiyama H, Horie M, Matsuzaki H, et al. TAZ contributes to pulmonary fibrosis by activating profibrotic functions of lung fibroblasts. *Sci Rep* 2017;7:42595.
- Robinson JT, Thorvaldsdóttir H, Winckler W, Guttman M, Lander ES, Getz G, et al. Integrative genomics viewer. *Nat Biotechnol* 2011;29:24–26.
- Subramanian A, Tamayo P, Mootha VK, Mukherjee S, Ebert BL, Gillette MA, et al. Gene set enrichment analysis: a knowledge-based approach for interpreting genome-wide expression profiles. *Proc Natl Acad Sci USA* 2005;102:15545–15550.
- Stuart T, Butler A, Hoffman P, Hafemeister C, Papalexi E, Mauck WM III, et al. Comprehensive integration of single-cell data. *Cell* 2019; 177:1888–1902, e21.
- Horie M, Saito A, Mikami Y, Ohshima M, Morishita Y, Nakajima J, et al. Characterization of human lung cancer-associated fibroblasts in three-dimensional *in vitro* co-culture model. *Biochem Biophys Res Commun* 2012;423:158–163.
- Horie M, Saito A, Yamauchi Y, Mikami Y, Sakamoto M, Jo T, et al. Histamine induces human lung fibroblast-mediated collagen gel contraction via histamine H1 receptor. *Exp Lung Res* 2014;40: 222–236.
- Okuda K, Chen G, Subramani DB, Wolf M, Gilmore RC, Kato T, et al. Localization of secretory mucins MUC5AC and MUC5B in normal/healthy human airways. *Am J Respir Crit Care Med* 2019;199: 715–727.
- Forrest AR, Kawaji H, Rehli M, Baillie JK, de Hoon MJ, Haberle V, et al.; FANTOM Consortium and the RIKEN PMI and CLST (DGT). A promoter-level mammalian expression atlas. *Nature* 2014;507:462–470.
- Hrycaj SM, Marty-Santos L, Cebrian C, Rasky AJ, Ptaschinski C, Lukacs NW, et al. *Hox5* genes direct elastin network formation during alveologenesis by regulating myofibroblast adhesion. *Proc Natl Acad Sci USA* 2018;115:E10605–E10614.
- ENCODE Project Consortium. An integrated encyclopedia of DNA elements in the human genome. *Nature* 2012;489:57–74.
- Sloan CA, Chan ET, Davidson JM, Malladi VS, Strattan JS, Hitz BC, et al. ENCODE data at the ENCODE portal. *Nucleic Acids Res* 2016; 44:D726–D732.
- Cordenonsi M, Zanconato F, Azzolin L, Forcato M, Rosato A, Frasson C, et al. The Hippo transducer TAZ confers cancer stem cell-related traits on breast cancer cells. *Cell* 2011;147:759–772.
- Tadokoro T, Gao X, Hong CC, Hotten D, Hogan BL. BMP signaling and cellular dynamics during regeneration of airway epithelium from basal progenitors. *Development* 2016;143:764–773.
- Chung MI, Bujinis M, Barkauskas CE, Kobayashi Y, Hogan BLM. Niche-mediated BMP/SMAD signaling regulates lung alveolar stem cell proliferation and differentiation. *Development* 2018;145:dev163014.
- Green J, Endale M, Auer H, Perl AK. Diversity of interstitial lung fibroblasts is regulated by platelet-derived growth factor receptor  $\alpha$  kinase activity. *Am J Respir Cell Mol Biol* 2016;54:532–545.
- Noskovičová N, Petřek M, Eickelberg O, Heinzlmann K. Platelet-derived growth factor signaling in the lung: from lung development and disease to clinical studies. *Am J Respir Cell Mol Biol* 2015;52:263–284.
- Ostman A, Heldin CH. PDGF receptors as targets in tumor treatment. *Adv Cancer Res* 2007;97:247–274.
- Schafer MJ, White TA, Iijima K, Haak AJ, Ligresti G, Atkinson EJ, et al. Cellular senescence mediates fibrotic pulmonary disease. *Nat Commun* 2017;8:14532.

43. Dong Y, Geng Y, Li L, Li X, Yan X, Fang Y, *et al.* Blocking follistatin-like 1 attenuates bleomycin-induced pulmonary fibrosis in mice. *J Exp Med* 2015;212:235–252.
44. Koli K, Myllärniemi M, Vuorinen K, Salmenkivi K, Ryyänänen MJ, Kinnula VL, *et al.* Bone morphogenetic protein-4 inhibitor gremlin is overexpressed in idiopathic pulmonary fibrosis. *Am J Pathol* 2006; 169:61–71.
45. Kondo A, Kaestner KH. Emerging diverse roles of telocytes. *Development* 2019;146:dev175018.
46. Popescu LM, Gherghiceanu M, Suciu LC, Manole CG, Hinescu ME. Telocytes and putative stem cells in the lungs: electron microscopy, electron tomography and laser scanning microscopy. *Cell Tissue Res* 2011;345:391–403.
47. Kaestner KH. The intestinal stem cell niche: a central role for Foxl1-expressing subepithelial telocytes. *Cell Mol Gastroenterol Hepatol* 2019;8:111–117.
48. Hussein MM, Mokhtar DM. The roles of telocytes in lung development and angiogenesis: an immunohistochemical, ultrastructural, scanning electron microscopy and morphometrical study. *Dev Biol* 2018;443:137–152.
49. Nabhan AN, Brownfield DG, Harbury PB, Krasnow MA, Desai TJ. Single-cell Wnt signaling niches maintain stemness of alveolar type 2 cells. *Science* 2018;359:1118–1123.
50. Kulkarni T, de Andrade J, Zhou Y, Luckhardt T, Thannickal VJ. Alveolar epithelial disintegrity in pulmonary fibrosis. *Am J Physiol Lung Cell Mol Physiol* 2016;311:L185–L191.